Plasma Shielding with a Rotating Magnetic Field for a Space Elevator

Toshiki TAKAHASHI, Hiroki SHIONOYA, Hirotomo ITAGAKI and Tomohiko ASAI

Department of Electronic Engineering, Gunma University, 1-5-1Tenjin-Cho, Kiryu 376-8515, Japan

College of Science and Technology, Nihon University, Tokyo 101-8308, Japan

(Received: 30 October 2009 / Accepted: 2 April 2010)

Plasma shielding with a rotating magnetic field from high-energy protons and electrons in the Van Allen radiation belts is numerically studied for a space elevator that is proposed as a future transportation system. Orbits of space electrons in the rotating magnetic field are calculated, and the density and flow velocity are estimated by a particle-in-cell method. It is found that the electron current can be driven successfully. However, the axial inductive electric field enhances axial acceleration of the electrons, which can result in radial electric field generation. High energy particle shielding by the poloidal magnetic field generated by the toroidal electron ring current is also studied with a concept of the Störmer region. In order to shield 1-MeV electrons in the radiation belts, electron density higher than 10^{13} m^{-3} is found to be needed.

Keywords: space elevator, plasma shielding, rotating magnetic field, particle-in-cell method, Störmer region

1. Introduction

A space elevator is a promising future transportation system and now being developed. The elevator climbs up along a cable from the earth surface to a station on the geostationary orbit. 90%-reduction of the transportation cost per unit weight to a space shuttle is obtainable. However, there are several issues to reach a practical application. According to a force balance calculation, a strong cable material is required to sustain a few GPa tension. Also, a climber must pass through two radiation belts called the Van Allen belts, where high-energy charged particles are present. The width of the inner and the outer radiation belts are about 3000 km and 10000 km, respectively. So the travel time across the radiation belts is estimated to excess a few days, and exposure to high-energy particles can damage not only electronically sensitive machine but also climber materials, and human body. To prevent from exposure of high-energy particles, conventional metal and/or water shielding are proposed. However, high-energy protons of over a few MeV activate metal material due to nuclear reaction. Also, an elevator gets heavier and the operation costs will increase.

A use of plasma shielding (magnetic shielding) can avoid proton bombardment. Power supply for plasma shielding is needed only when a climber passes through the Van Allen belts. Since the electron density is estimated to be 10^{10} m^{-3} in the radiation belts, the shielding plasma is available.

A rotating magnetic field (RMF) method is widely spread in the compact torus (CT) plasma research community to drive the electron current of the CT plasma [1, 2], and it is efficient to prolong the life time of the field-reversed configuration plasma from a few micro-seconds to at most 10 milli-seconds [3]. The RMF generated by the axial alternating current has a radial component that rotates azimuthally with a higher angular frequency than the ion cyclotron frequency and with a lower one than the electron cyclotron frequency. Then, electrons alone can follow the rotating field, and on the other hand ions can not follow it and stay still. We propose here magnetic shielding for a space elevator in which the RMF drives the electron azimuthal motion to generate the poloidal magnetic field.

To verify the concept of the plasma shielding with RMF, an experimental setup has now been ready at Nihon University [4]. Comparison between experimental and computational study on RMF current drive efficiency is now required, and it is important to find shielding ability to protect a space elevator.

2. Electron current drive by the rotating magnetic field

In the present calculation, four RMF antennae are set around an elevator; those locations are shown in Fig. 1. The phase of each antenna current shifts 90 degrees each other and the current can be written in

$$I_n = I_0 \sin(\omega_{\mathrm{RMF}} t + n\pi/2), \quad n = 0,1,2,3$$

author's e-mail:t-tak@el.gunma-u.ac.jp

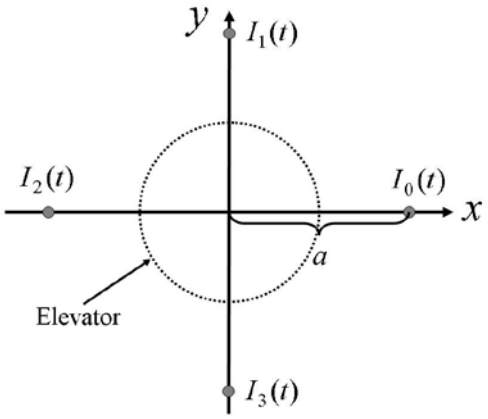

Fig.1 Geometry of four RMF antennae and the elevator, where a is the radial distance from the origin to the antenna.

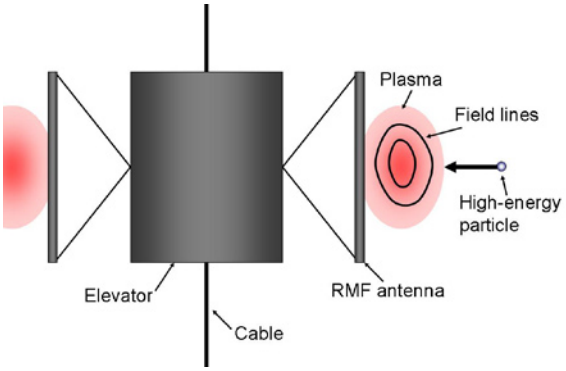

Fig.2 Side view of a space elevator with a plasma shield and schematic diagram of high-energy particle injection.

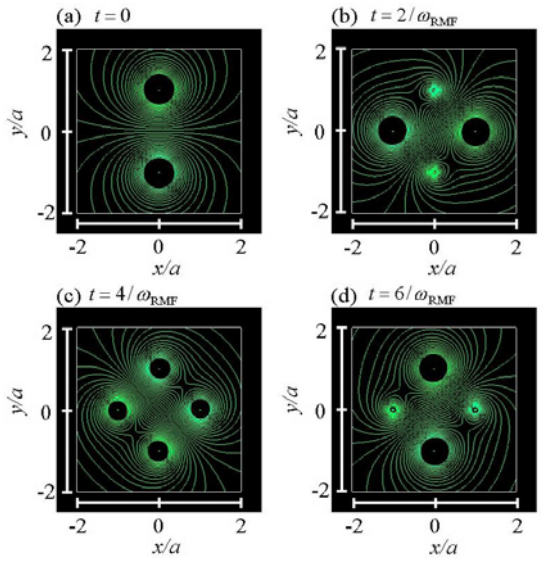

Fig.3 Temporal change of the contour lines of axial vector potential; the lines are identical with the field lines.

Table 1 Calculation parameters

Electron density n_0 [m^{-3}]	10^{10}
Electron temperature T_e [eV]	1
RMF antenna position a [m]	10
Axial length of RMF antenna [m]	10
Peak current of antenna I [kA]	5

where ω_{RMF} is the angular frequency of the RMF. The current generates the magnetic field, and we calculate it together with the axial vector potential A_z in the vacuum space. Side view of proposed plasma shielding system is presented in Fig. 2. The RMF antenna length is set to be the same as the elevator length here. Incident high-energy particles along the cable can not be shielded in the present magnetic configuration. We need to modify arrangement of the RMF antenna and configuration of the shielding plasma in the next step study.

Trajectories of electrons in the vacuum field are calculated by integrating numerically the equation of motion:

$$m_e \frac{d\mathbf{v}}{dt} = -e(\mathbf{E} + \mathbf{v} \times \mathbf{B}).$$

Here, the magnetic field $\mathbf{B}$ is generated by the RMF antenna and $\mathbf{E}$ is the inductive electric field given by

$$E_z = -\frac{\partial A_z}{\partial t}.$$

Evolution of the RMF in almost one cycle and in the x-y plane is shown in Fig. 3. In the real situation, a space elevator is located at around the origin of Fig. 3, and therefore the effect of its metal wall prevents the magnetic field from penetrating in the elevator. Here, we neglect deformation of the magnetic field by presence of an elevator and plan to study it in near future. The initial position of an electron is given by the uniform random number in 3-dimensional space, and its velocity is chosen from the Maxwell distribution numerically. In this calculation, we calculate orbits of 50,000 electrons. The electron density and flow velocity are calculated by a PIC method. The parameters used here are summarized in Table. 1. These values are almost the same as those in [4]. The toroidal electron current ring generates the poloidal magnetic field, and the electron motion is restricted by both the RMF and poloidal field. So, a self-consistent magnetohydrodynamic calculation is needed to reproduce the RMF driven plasma; it is neglected here. Objectives of the present paper are to estimate the RMF electron current drive efficiency by a simple calculation and to investigate feasibility of high-energy particle shielding by the generated magnetic field.

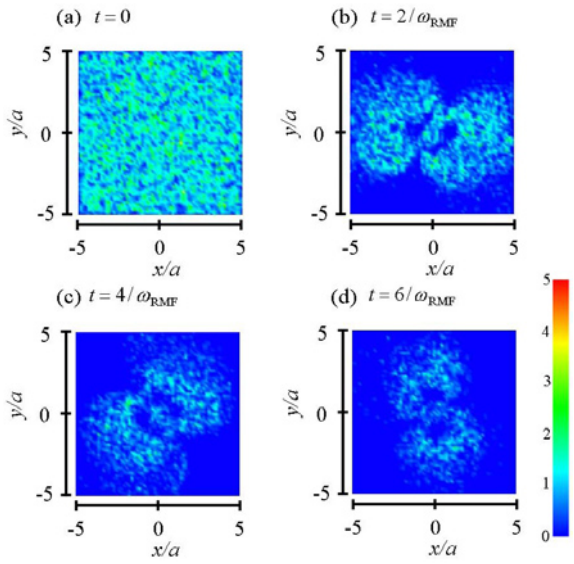

Fig.4 The color contour of the electron density just after application of the antenna current at (a) $t=0$, (b) $t=2/\omega_{\mathrm{RMF}}$, (c) $t=4/\omega_{\mathrm{RMF}}$, and (d) $t=6/\omega_{\mathrm{RMF}}$. The value of density is normalized by n_0.

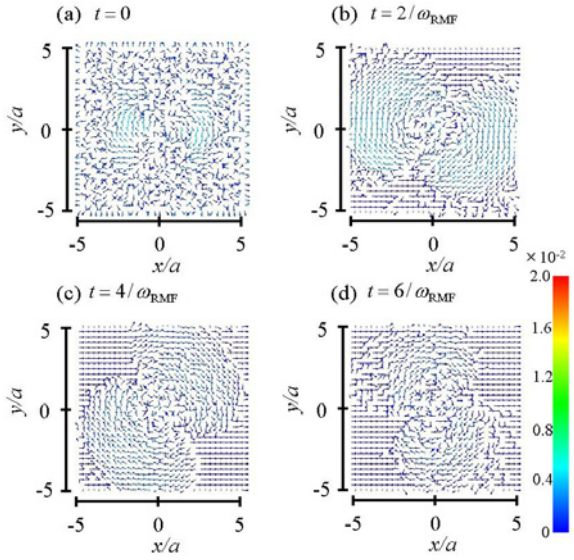

Fig.5 The vector plot of the electron flow velocity. The color indicates the magnitude of velocity that is normalized by a/τ.

The time evolutions of the electron density and flow velocity are shown in Figs. 4 and 5, where the RMF angular frequency is $\omega_{\mathrm{RMF}}\tau=10^{-3}$, $\tau\equiv m_{\mathrm{e}}/(qB_0)$, and $B_0\equiv\mu_0 I_0/(4\pi a)$. In this case the RMF frequency is relatively lower than the electron cyclotron frequency. We can clearly see rotating motion of the electron fluid from both Figs. 4 and 5. It is found that the total number of electrons, however, gradually decrease, and at $t=6/\omega_{\mathrm{RMF}}$ remaining electrons in the calculation box is

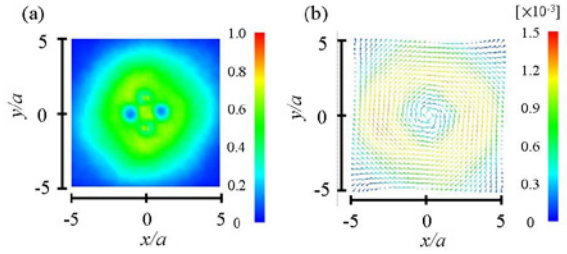

Fig.6 Time-averaged two dimensional profiles. (a) The color contour of electron density profile and (b) the vector plot of flow velocity. (a) and (b) are drawn in the same manner as Figs. 4 and 5, respectively.

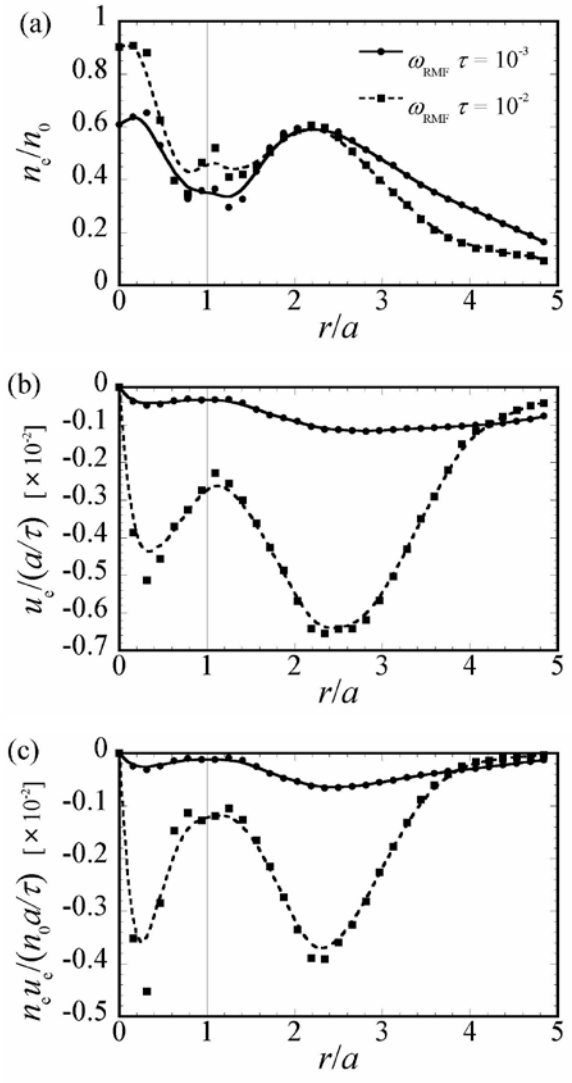

Fig.7 The time-averaged radial profiles of (a) the electron density, (b) flow velocity, and (c) flux. The solid line is for the RMF angular frequency of $\omega_{\mathrm{RMF}}\tau=10^{-3}$, and the dashed line is for $\omega_{\mathrm{RMF}}\tau=10^{-2}$. The curves are drawn smoothly to guide the reader's eye.

less than initial electrons. According to calculation of a single particle orbit, an electron near the antenna is accelerated in the axial direction by the inductive electric field. The accelerated electron goes to weaker magnetic field region and at last is lost away from the calculation region. Since a faster electron loss rate results in the radial ambipolar electric field in order to keep charge neutrality, the rapid decrease in the electron density observed here is suppressed in a real experiment.

Figures 4 and 5 show a transient process. To find the time-averaged profile, we calculate the time-averaged quantity $\langle X(\mathbf{r})\rangle$ of the time-varying quantity $X(\mathbf{r},t)$ over one period of the RMF as

$$\langle X(\mathbf{r})\rangle \equiv \frac{\omega_{\mathrm{RMF}}}{2\pi}\int_0^{2\pi/\omega_{\mathrm{RMF}}} X(\mathbf{r},t)\,\mathrm{d}t\,.$$

The time-averaged electron density and flow velocity are shown in Fig. 6 (a) and (b), respectively. It is found that the toroidal electron ring current is successfully driven in the same direction as the RMF. The toroidal plasma is found to exist in $r/a \le 5$ and be absent near the antenna.

Obtained radial profiles of the time-averaged electron density, flow velocity, and flux are shown in Fig. 7 for $\omega_{\mathrm{RMF}}\tau = 10^{-2}$ and 10^{-3}. We can see clearly the peak of the flow velocity at $r = 2.5a$ for $\omega_{\mathrm{RMF}}\tau = 10^{-2}$. For the lower frequency case of $\omega_{\mathrm{RMF}}\tau = 10^{-3}$, the profile shows the flat top and the density is relatively high contrary to the case that $\omega_{\mathrm{RMF}}\tau = 10^{-2}$. We also find another peak of the flux within the antenna position and near the elevator. This peak can be neglected in a realistic case, because of deformation of the magnetic field due to presence of the elevator. It is found from a peaked profile seen in Fig. 7 (c) that the RMF can form the ring current encircling the elevator.

If electrons can follow completely the RMF field, the electron flow velocity becomes $u_{\mathrm{e}\theta} = r\omega_{\mathrm{RMF}}$; it is the rigid rotor profile. We define the RMF current drive efficiency η as

$$\eta \equiv \frac{(n_{\mathrm{e}}u_{\mathrm{e}\theta})_{\max}}{(n_{\mathrm{e}}r\omega_{\mathrm{RMF}})_{\max}}\,.$$

The subscript "max" means the peak value. The frequency dependence of η is presented in Fig. 8. The efficiency η is found to decrease with the RMF frequency. The fitting curve becomes

$$\eta \approx 0.4\exp(-33.7\omega_{\mathrm{RMF}}\tau)\,.$$

It appears that the RMF slips in the higher frequency range. For a detailed calculation of the current drive efficiency, however, penetration of the RMF into the plasma and the plasma response [5] should be considered; these issues will be investigated in our future study.

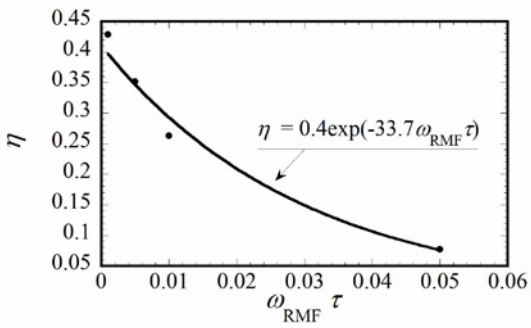

Fig.8 The frequency dependence of RMF current drive efficiency η.

3. Accessibility of a high-energy charged particle in the shielding field

We will discuss here accessibility of high-energy charged particles in the magnetic field generated by the RMF. Assuming the electron current has only the toroidal component and is axisymmetrically distributed, we obtain the poloidal flux function by solving the following partial differential equation:

$$r\frac{\partial}{\partial r}\left(\frac{1}{r}\frac{\partial \psi}{\partial r}\right) + \frac{\partial^2 \psi}{\partial z^2} = -\mu_0 r j_{\mathrm{e}\theta}\,. \qquad (1)$$

We solved Eq. (1) by means of the finite difference method. The radial and axial magnetic field components are

$$B_r = -\frac{1}{r}\frac{\partial \psi}{\partial z},\quad B_z = \frac{1}{r}\frac{\partial \psi}{\partial r}\,.$$

From the flow velocity profile shown in Fig. 7, we assume the profile of the electron current density and set analytically in the form:

$$j_{e\theta}(r,z) = -4 j_{\theta\max}\frac{(r-r_{\mathrm{out}})(r-r_{\mathrm{in}})}{(r_{\mathrm{out}}-r_{\mathrm{in}})^2}\exp(-z^2/2\sigma^2)\,. \quad (2)$$

Here, $j_{\theta\max}$, r_{out}, r_{in}, and σ are the constant parameters to control the ring current and its profile. The obtained poloidal flux is shown in Fig. 7(c), where $j_{\theta\max} = I/(8\pi a^2) \approx 2.0$ [A/m^2], $r_{\mathrm{out}} = 5a = 50$ [m], $r_{\mathrm{in}} = 0.5a = 5$ [m], and $\sigma = 0.5a = 5$ [m], respectively. Here, the axial electron density is in the Gaussian distribution, and σ^2 is its variance. We set empirically the value of σ from the density profile in *r*-*z* plane obtained from the same calculation explained in Sec. 2. The poloidal magnetic field line (the contour of the poloidal flux) is shown in Fig. 9.

Now, we consider shielding ability of the magnetic field. Here we assume axisymmetry $\partial/\partial\theta = 0$. Suppose that a charged particle with the kinetic energy E and the canonical angular momentum P_θ approaches form infinity and enters perpendicularly to the elevator (i.e., *z*=0)as shown in Fig.2. In this case $P_\theta = 0$. Then, the

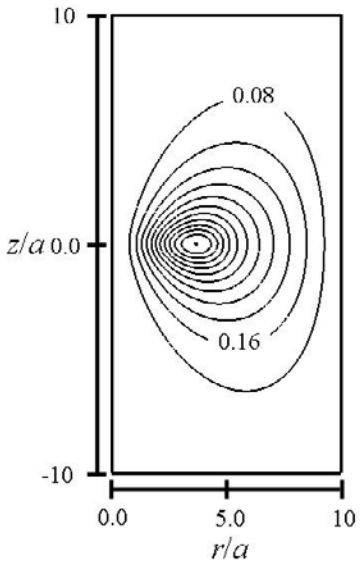

Fig.9 The contour lines of the poloidal flux function generated by the ring current.

particle with the charge q is accessible in the region where the following inequality satisfies:

$$E \geq \frac{(P_\theta - q\psi)^2}{2mr^2} = \frac{q^2\psi^2}{2mr^2}. \quad (3)$$

The magnetic field can shield the particle if its energy satisfies

$$E \leq \frac{q^2}{2m}\left(\frac{\partial\psi}{\partial r}\right)_0^2. \quad (4)$$

Here, the subscript 0 indicates a value at the position where

$$\left(\frac{\partial\psi}{\partial r}\right) = \frac{\psi(r)}{r}, \quad (5)$$

is satisfied. The position $r = r_0$ is the solution to Eq. (5).

The critical shielding energy depends on the constant parameters in Eq. (2). In particular, $j_{\theta\max}$ is the most sensitive parameter. We introduce a non-dimensional parameter as

$$\alpha \equiv \frac{\mu_0 e^2 a^2}{m_e}\left|\frac{j_{\theta\max}}{en_0 a/\tau}\right| n_0.$$

Here,

$$\left|\frac{j_{\theta\max}}{en_0 a/\tau}\right| \approx 0.4\times10^{-2},$$

for $\omega_{RMF}\tau = 10^{-2}$ as shown in Fig. 7 (c). In the case of $\omega_{RMF}\tau = 10^{-2}$, the relation between the critical shielding energy and α is presented in Fig. 10. Note that Fig. 10 is applicable only to particles moving toward $(r,z) = (r_0, 0)$ (See Fig. 2). The parameter α depends also on the electron density, and its value is indicated at the top of the figure. In this figure, we calculate the critical energy of high-energy electrons and protons in the Van Allen radiation belts. It is found that the electron density of 10^{13} m^{-3} is required in order to shield 1-MeV electrons.

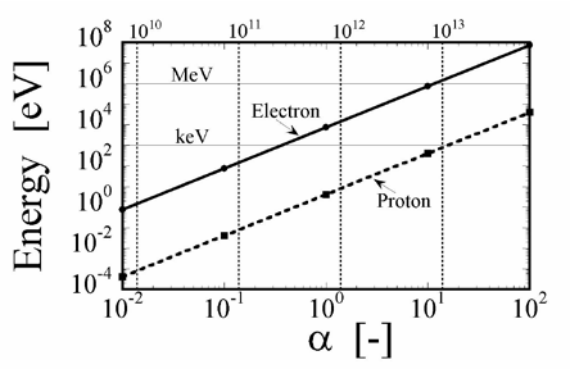

Fig.10 The critical shielding energy for electrons (solid line) and protons (dashed line) versus the non-dimensional RMF current parameter α.

4. Summary

We have investigated possibility of the electron current drive by means of a rotating magnetic field (RMF). The ring current encircling the elevator generates the poloidal magnetic field to shield high-energy charged particle in the Van Allen radiation belts and to protect sensitive devices and human in a space elevator. When the RMF angular frequency is 10^{-2} times lower than the typical electron cyclotron frequency, it is found that the electron current can by successfully driven. In order to shield 1-MeV electrons in the radiation belts, it is found that the electron density higher than at least 10^{13} m^{-3} is needed.

[1] J.T. Slough and K.E. Miller, Phys. Rev. Lett. **85**, 1444 (2000).
[2] H.Y. Guo *et al*., Phys. Plasmas **9**, 185 (2002).
[3] H.Y. Guo *et al*., Phys. Rev. Lett. **97**, 235002 (2006).
[4] H.Itagaki *et al*., Proceedings of 27th International Symposium Space Technology and Science, 2009-g-33.
[5] M. Ohnishi and A. Ishida, Phys. Plasmas **9**, 2633 (2002).